

Accurate masses of neutron-deficient nuclides close to $Z = 82$

S. Schwarz^{a,1,2} F. Ames^{b,c} G. Audi^d D. Beck^e G. Bollen^{b,2}
C. De Coster^{f,3} J. Dilling^e O. Engels^b R. Fossion^f
J.-E. Garcia Ramos^f S. Henry^d F. Herfurth^{e,b} K. Heyde^f
A. Kellerbauer^{a,g} H.-J. Kluge^e A. Kohl^e E. Lamour^e
D. Lunney^d I. Martel^h R. B. Moore^g H. Raimbault-Hartmann^c
C. Scheidenberger^e G. Sikler^e J. Szerypoⁱ C. Weber^e
and the ISOLDE Collaboration^a

^a*CERN, CH-1211 Geneva 23, Switzerland*

^b*Sektion Physik, Ludwig-Maximilians-Universität München, D-85748 Garching, Germany*

^c*Johannes Gutenberg Universität Mainz, Institut für Physik, D-55099 Mainz, Germany*

^d*CSNSM-IN2P3-CNRS, Bâtiment 108, F-91405 Orsay-Campus, France*

^e*GSI, Planckstr. 1, D-64291 Darmstadt, Germany*

^f*Dep. of Subatomic and Radiation Physics, Universiteit Gent, Proeftuinstraat 86, B-9000 Gent, Belgium*

^g*McGill University, Department of Physics, Montréal (Québec) H3A 2T8, Canada*

^h*Instituto de Estructura de la Materia, CSIC, Madrid, Spain*

ⁱ*Department of Physics, University of Jyväskylä, PB 35(Y5), FIN-40351 Jyväskylä, Finland*

Abstract

Mass measurements with the Penning trap mass spectrometer ISOLTRAP at ISOLDE/CERN are extended to non-surface ionizable species using newly developed ion beam bunching devices. Masses of $^{179-197}\text{Hg}$, $^{196,198}\text{Pb}$, ^{197}Bi , ^{198}Po and ^{203}At were determined with an accuracy of $1 \cdot 10^{-7}$ corresponding to $\delta m \approx 20$ keV. Applying a resolving power of up to $3.7 \cdot 10^6$ ground and isomeric states of $^{185,187,191,193,197}\text{Hg}$ were separated. First experimental values for the isomeric excitation energy of $^{187,191}\text{Hg}$ are obtained. A least-squares adjustment has been performed and theoretical approaches are discussed to model the observed fine structure in the binding energy.

PACS: 07.75.+h, 21.10.Dr, 27.70.+q, 27.80.+w, 32.10.Bi

Keywords: Radioactive Nuclides; Atomic Masses; Mass Spectrometry; Penning Trap; Mercury Isotopes

1 Introduction

The region of neutron-deficient isotopes of elements close to $Z = 82$ has been of considerable interest due to its very peculiar nuclear structure phenomena [1,2]. The huge shape transition [3] and odd-even staggering in charge radii [4] observed in optical spectroscopy experiments on mercury isotopes was explained by the phenomenon of nuclear shape coexistence [5,6]. These early measurements triggered a wealth of further theoretical and experimental studies in this region which give a quite complete picture of coexisting nuclear configurations, mixing of these configurations and on nuclear shapes. However, there was hardly any information available on the very fundamental property of these nuclides, namely their total binding energy.

In recent years, techniques for direct mass spectrometry on radioactive nuclides have been developed, which allow one also to access very short-lived nuclides produced in minute quantities. One of these techniques is Penning trap mass spectrometry, which is known from measurements on stable ions to deliver unprecedented accuracy [7]. ISOLTRAP [8,9] at the on-line mass separator ISOLDE at CERN is a tandem Penning trap mass spectrometer tailored for the study of short-lived nuclides. As in all Penning trap mass experiments, the mass determination is carried out via the determination of the cyclotron frequency $\nu_c = q/m \cdot B/2\pi$ of the ion with a charge-to-mass ratio q/m stored in a magnetic field B . The value of the latter is usually precisely obtained by a cyclotron frequency determination of an ion with a well known mass value. ISOLTRAP has been in operation since many years and about two hundred radioactive nuclides have been investigated. Due to the recent implementation of a system for ion beam accumulation, cooling and bunching based on a gas-filled radiofrequency (RFQ) ion trap [10], the applicability of ISOLTRAP was extended to all beams available at ISOLDE with sufficient intensity. This was the prerequisite for the measurements presented here.

In this paper we report on mass measurements of $^{179-197}\text{Hg}$, $^{196,198}\text{Pb}$, ^{197}Bi , ^{198}Po and ^{203}At . It should be mentioned that direct measurements in the $Z = 82$ region have also been carried out by Schottky mass spectrometry in a cooler storage ring [11]. In the cases where data from both experiments exist, there is good agreement. However, the ISOLTRAP data are typically five times more accurate than the storage ring data. The high accuracy of the ISOLTRAP data allows for a very detailed study of the fine structure in the trend of binding energies far from stability.

¹ Corresponding author, tel: xx1-517-333-6442, fax: xx1-517-353-5967, e-mail: schwarz@nscl.msu.edu

² Present address: NSCL/MSU, South Shaw Lane, East Lansing 48824, Michigan, USA

³ Postdoctoral research fellow of the Fund for Scientific Research (FWO)- Flanders (Belgium)

2 Experimental procedure

In the measurements the 60-keV ISOLDE ion beam was injected into the RFQ ion cooler system, which is placed on a potential near to 60 kV. Accumulated ions are released again as short ion bunches with about 2 keV kinetic energy. By employing a pulsed cavity the potential energy of the ions is reduced to zero and the low-energy ions are transferred into a first Penning trap. This system uses a mass selective buffer gas cooling technique and is able to purify the ISOLDE ion bunches from isobaric contaminations before they are delivered to a precision trap. Here the cyclotron frequency is determined by driving the ion motion with an azimuthal quadrupole RF field of frequency ν_d for a period T_d and by applying a time-of-flight resonance detection technique, which is based on the adiabatic conversion of gained radial energy into axial energy. A cyclotron resonance curve is obtained by ejecting the ions from the trap and determining their time-of-flight to an ion detector as a function of the RF frequency. For $\nu_d = \nu_c$, a reduction of the time-of-flight is observed. The line width $\Delta\nu(\text{FWHM}) \approx 1/T_d$ of the resonance curve and hence the mass resolving power $R = \nu_c/\Delta\nu(\text{FWHM}) = m/\Delta m$ are directly determined by the RF excitation time T_d .

3 Experimental results

The results discussed in this paper have been collected in a series of five runs. For the production of the radioactive nuclides four molten lead targets (runs #1-3,5) and a thorium-carbide target (run #4) with plasma ion sources were used. ^{208}Pb was used as the reference nuclide for all the mass measurements reported here except for $^{184,186}\text{Hg}$, where ^{204}Pb was chosen.

The experimental results of a measurement with ISOLTRAP are the ratios of the cyclotron resonance frequency of the investigated nuclides to that of the chosen reference nuclide. By fitting the theoretical line shape [12] to the cyclotron resonance curves, cyclotron frequencies are obtained together with their statistical errors. Figure 1(a) shows the cyclotron resonance curve taken with $T_d = 8$ s for ^{208}Pb together with a fit of the theoretical line shape. If there is evidence that no “contaminating” ions influence the measurement of the cyclotron resonance (as is the case in Fig. 1(a)) the mass ratios can directly be calculated from the resonance frequencies. Effects of contamination were observed for the data on odd Hg isotopes since many of these isotopes are produced at ISOLDE in the ground state as well as in the isomeric state.

The isomeric excitation energies of the odd-N isotopes $^{183-197}\text{Hg}$ are lower than 300 keV [13]. In the first run $T_d = 0.9$ s was chosen resulting in a mass

resolving power of $m/\Delta m = 4 \cdot 10^5$. At mass number $A = 190$ this results in a mass resolution of 475 keV, insufficient to resolve the ground and isomeric states. If the two resonances cannot be resolved, one single cyclotron resonance curve is obtained the center of which corresponds to the average mass of the ions in the trap [14]. In the subsequent runs T_d was increased up to 8 s resulting in a resolving power of up to $R = m/\Delta m = 3.7 \cdot 10^6$ and a mass resolution of down to 49 keV, respectively. Isomeric and ground states could be separated for $^{185,187,191,193,197}\text{Hg}$ thereby allowing the direct determination of the ground state mass. As an example figure 1(b) depicts the cyclotron resonance curve taken with $T_d = 8$ s for ^{185}Hg . The two states are clearly resolved. The solid curve shows a fit of the theoretical line shape to the data, which is a superposition of two cyclotron resonance curves [12].

All the resonance curves for the odd Hg-isotopes were recorded with an average number of detected ions of $\bar{n} = 3-8$ in a single time-of-flight (TOF) spectrum. Only ^{197}Hg was studied with $\bar{n} = 32$ which may have caused frequency shifts due to Coulomb interaction of ions with different mass (see below).

Table 1 lists the frequency ratios obtained with ISOLTRAP. For repeated measurements in runs #1 to #4 weighted averages of the frequency ratios are given. Data obtained in run #5 (fall 2000) are listed separately, because they were taken after a mass evaluation was completed which includes the combined data from runs #1 to #4 (see discussion below). For the mercury isotopes marked by g or m the two states were resolved and both frequency ratios were obtained by fitting a superposition of two cyclotron resonance curves to the data. In the case of ^{195}Hg (signaled by x) the mass resolving power was insufficient to resolve ground state from isomeric state.

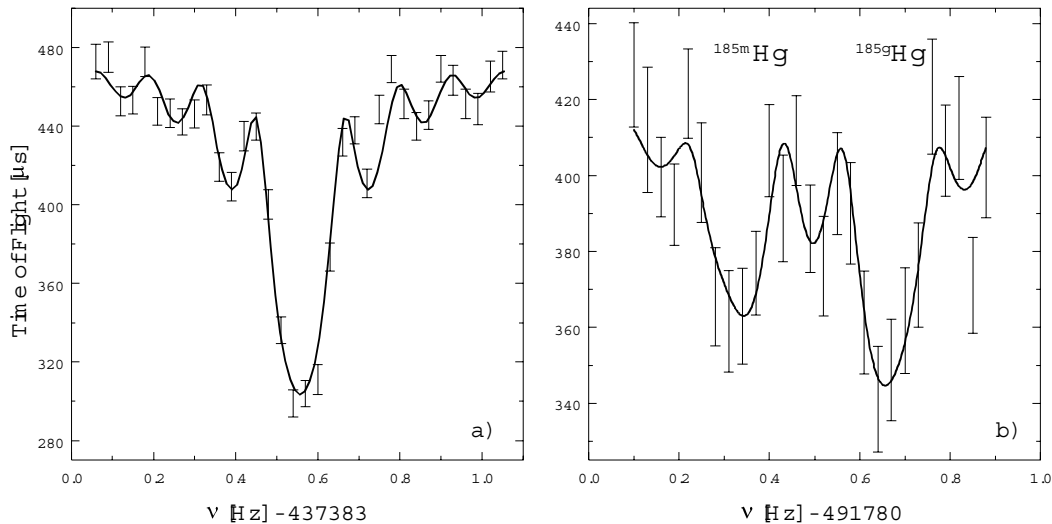


Fig. 1. Cyclotron resonances for ^{208}Pb (a) and $^{185g,185m}\text{Hg}$ ions (b) obtained with excitation time $T_d = 8$ s. The solid curves are the theoretical line shapes [12] fitted to the data.

Table 1

Ratios of the cyclotron frequencies of reference isotopes ν_{ref} to those of investigated isotopes ν . Column 4 indicates the excitation times T_d applied in the runs listed in column 2. The errors given in round and square brackets are the statistical and total uncertainty, respectively. For repeated measurements in runs #1 to #4 column 5 lists weighted averages of the ratios.

Isotope	Run	Ref.	T_d [s]	ν_{ref}/ν
^{182}Hg	3	^{208}Pb	0.9	0.874976142 (33) [94]
^{183}Hg	3	^{208}Pb	0.9,2,4	0.879783270 (22) [91]
^{184}Hg	2	^{204}Pb	0.9	0.901940975 (40) [99]
^{185g}Hg	2	^{208}Pb	8	0.889387382 (11) [90]
^{185m}Hg	2	^{208}Pb	8	0.889388002 (17) [91]
^{186}Hg	2	^{204}Pb	0.9	0.911734701 (34) [97]
^{187g}Hg	3	^{208}Pb	5	0.898993914 (28) [94]
^{187m}Hg	3		5	0.898994193 (23) [93]
^{188}Hg	1		0.9	0.903791407 (28) [95]
^{189m}Hg	4		8	0.908603074 (31) [96]
^{190}Hg	1		0.9	0.913401926 (23) [94]
^{191g}Hg	2		8	0.918214162 (30) [97]
^{191m}Hg	2		8	0.918214821 (17) [93]
^{192}Hg	1		0.9	0.923015056 (22) [95]
^{193g}Hg	2		8	0.927828286 (10) [93]
^{193m}Hg	2		8	0.927828968 (19) [95]
^{194}Hg	1,2,3		0.9,8	0.932630714 (09) [94]
^{195x}Hg	1		0.9	0.937445251 (23) [97]
^{196}Hg	1		0.9	0.942249017 (27) [98]
^{197g}Hg	2		4	0.947063981 (27) [99]
^{197m}Hg	2		4	0.947065345 (89)[130]
^{200}Hg	1	^{208}Pb	0.9	0.961494050 (97)[137]
^{179}Hg	5	^{208}Pb	0.9	0.860585642(140)[164]
^{180}Hg	5		0.9	0.865376757 (65)[108]
^{181}Hg	5		0.9	0.870182713(172)[193]
^{182}Hg	5		0.9	0.874976120 (46) [99]
^{183}Hg	5		0.9,2,5,5	0.879783305 (12) [89]
^{184}Hg	5	^{208}Pb	0.9	0.884578398 (28) [93]
^{196}Pb	4	^{208}Pb	0.9	0.942282439 (45)[105]
^{198}Pb	4		0.9	0.951895304 (54)[110]
^{204}Pb	2	^{208}Pb	0.9	0.980749697 (27)[102]
^{197}Bi	4	^{208}Pb	0.9,4	0.947119980 (43)[104]
^{198}Po	4	^{208}Pb	0.9	0.951949947 (65)[115]
^{203}At	4	^{208}Pb	0.9	0.976008061 (69)[119]

Table 2

Isomeric excitation energies E_{isol} as obtained by ISOLTRAP together with literature values E_{lit} [13]. In the case of E_{isol} only the statistical uncertainty is given. Literature values marked by # are estimates based on systematic trends.

Isomer	Excitation Energy [keV]		Difference [keV]
	E_{isol}	E_{lit}	$E_{isol} - E_{lit}$
^{185m}Hg	120 (5)	103.8 (1.0)	16
^{187m}Hg	54 (7)	100 (70) #	
^{191m}Hg	128 (8)	140 (50) #	
^{193m}Hg	132 (6)	140.76 (5)	-8
^{197m}Hg	264 (18)	298.93 (8)	-35

The error given is the statistical uncertainty; it is typically $\delta\nu/\nu = 4 \cdot 10^{-8}$ for the nuclides studied with $T_d = 0.9$ s and for a few thousand registered ions. For $T_d = 8$ s this decreases to $\delta\nu/\nu = 1 \cdot 10^{-8}$. In the cases of $^{179,181,200}\text{Hg}$ less than 300 ions were detected resulting in $\delta\nu/\nu \approx 1 \cdot 10^{-7}$.

The uncertainty in calibrating the magnetic field B gives the main contribution to the systematic error. On top of a nearly linear decrease of $\Delta B/B = 1 \cdot 10^{-7}$ per day, short-term variations with a standard deviation of $\sigma \approx 3 \cdot 10^{-8}$ are observed. Taking other smaller systematic effects like those due to trapping field imperfections into account results in a conservative estimate for the systematic error of $1 \cdot 10^{-7}$. Adding this quadratically to the statistical error gives the total error of the ISOLTRAP measurements (error values in square brackets in Table 1).

An outstanding result of this work is the fact that for $^{185,187,191,193,197}\text{Hg}$ isomeric and ground states are resolved. Beside the exciting feature of directly determining the energy E of the isomeric state with respect to the ground state, the most important result is, that the ground state mass can be determined unambiguously. The energy of the isomer can be directly extracted from the measured cyclotron frequency ratios of both states (Table 1) and the mass of the reference isotope ^{208}Pb [15]. E_{isol} as determined by ISOLTRAP is given in Table 2 together with literature values E_{lit} [13] as far as available. In the cases of $^{187m,191m}\text{Hg}$ the previously unknown energy of the isomers was determined for the first time. For ^{193m}Hg the ISOLTRAP values agree fairly well with the adopted excitation energies. For ^{197m}Hg a larger deviation of nearly 2σ (statistical error) is observed, possibly due to the high countrate used in this measurement. In the case of ^{185m}Hg , E_{isol} deviates by 3σ from E_{lit} . The adopted value E_{lit} is the sum of three decay energies obtained in two different spectroscopy experiments [16,17]. The difficulties in assigning the observed spectra to states and the fact that three individual measurements contribute to the energy of the isomer have to be balanced against the straightforward determination by ISOLTRAP. Since a very low count rate was used, contamination effects can practically be excluded. The energy of the isomer should

be even larger if such effects were present. Hence, the ISOLTRAP value can be expected to be very close to the true value for the energy of the isomeric state.

4 Mass evaluation

In order to make best use of the ISOLTRAP data and to obtain mass values relying on all relevant data, the available information on nuclear masses (e.g. Q-values, frequency ratios etc.) is cast into a network of linear mass relations and solved via a least squares adjustment. This procedure (called Atomic Mass Evaluation, AME) is repeated regularly [15,18]. To integrate the results reported here an intermediate adjustment was performed including the ISOLTRAP data then available (i. e. runs #1 to #4). Before discussing its outcome some special cases need to be addressed.

In order to account for a possibly still unrecognized systematic error in evaluating cases with isomeric and ground state resolved, an additional error of 20 keV is added quadratically to the errors of the input values for $^{185,191,193,197}\text{Hg}$.

In the case of ^{183}Hg no indication for a significant production of both nuclear states was found and only a single resonance was observed which is tentatively assigned to the ground state.

The spectra of ^{189}Hg taken with high resolving power are dominated by the resonance due to the isomeric state. A contribution from the ground state is noticed but it is too small to directly extract its cyclotron frequency. However, combining the results obtained with different resolving power allow for an estimate of the excitation energy $E(^{189}\text{Hg}) = 100(50)$ keV.

Due to lack of time ^{195}Hg could not be investigated with high resolving power. Hence a center-of-gravity resonance of the ion mixture was observed. However, additional information is available that can be used to obtain a reliable value for the ground state mass. In spectroscopic studies accompanying the mass measurements a ratio $R = Y_m/Y_g = 0.3(2)$ for the production of ions in the isomeric and of the ground state was found. Together with the literature value for the excitation energy $E_{lit} = 176.07(4)$ keV [13] a correction [19] $m_{mix} - m_g = E_{lit} \cdot R/(1 + R) = 40(20)$ keV can be calculated. Together with the frequency ratio from Table 1 this correction for the ground state mass of ^{195}Hg is taken as input data for the mass adjustment.

The final result of the Atomic Mass Evaluation for those nuclides investigated by ISOLTRAP is compiled in Table 3. Mass values listed in column 2 are calculated using frequency ratios from Table 1 and the reference mass data

Table 3

Results for the mass excess values for the nuclides investigated by ISOLTRAP. The values in column 2 are calculated using the frequency ratios from Table 1 and mass data for the reference isotopes from the new atomic mass adjustment. The result of the adjustment is given in column 3. All errors include statistical and systematic uncertainties. The last column gives the influence of the Penning trap data on the mass excesses given in column 3. The label “U” indicates cases where the ISOLTRAP results were not used in the adjustment due to the availability of better literature values. Data listed in the last six rows were obtained in run #5 after completion of the mass adjustment (cf. Table 1).

Nuclide	Mass excess [keV]		Influence [%]
	ISOLTRAP	AME new	
¹⁸² Hg	-23601 (18)	-23600 (18)	100
¹⁸³ Hg	-23817 (18)	-23817 (18)	100
¹⁸⁴ Hg	-26373 (19)	-26374 (19)	100
¹⁸⁵ Hg	-26215 (27)	-26215 (27)	100
¹⁸⁶ Hg	-28562 (19)	-28561 (19)	99
¹⁸⁷ Hg	-28144 (18)	-28144 (19)	100
¹⁸⁸ Hg	-30227 (19)	-30228 (19)	100
¹⁸⁹ Hg	-29664 (53)	-29664 (53)	100
¹⁹⁰ Hg	-31385 (18)	-31384 (16)	73
¹⁹¹ Hg	-30611 (30)	-30617 (27)	90
¹⁹² Hg	-32035 (19)	-32035 (19)	100
¹⁹³ Hg	-31069 (29)	-31070 (16)	36
¹⁹⁴ Hg	-32196 (18)	-32215 (14)	63
¹⁹⁵ Hg	-31017 (30)	-31031 (24)	89
¹⁹⁶ Hg	-31846 (19)	-31843 (4)	U
¹⁹⁷ Hg	-30543 (30)	-30557 (4)	U
²⁰⁰ Hg	-29511 (27)	-29520 (3)	U
¹⁹⁶ Pb	-25371 (20)	-25371 (21)	100
¹⁹⁸ Pb	-26073 (21)	-26073 (22)	100
²⁰⁴ Pb	-25120 (20)	-25123 (3)	U
¹⁹⁷ Bi	-19696 (20)	-19695 (21)	100
¹⁹⁸ Po	-15487 (22)	-15487 (18)	61
²⁰³ At	-12216 (23)	-12214 (23)	98
¹⁷⁹ Hg	-16969 (32)		
¹⁸⁰ Hg	-20287 (21)		
¹⁸¹ Hg	-20731 (37)		
¹⁸² Hg	-23605 (19)		
¹⁸³ Hg	-23811 (17)		
¹⁸⁴ Hg	-26359 (18)		

$ME(^{204}\text{Pb}) = -25122.9(2.9)$ keV and $ME(^{208}\text{Pb}) = -21763.0(2.9)$ keV from the new adjustment. For ^{189,195}Hg the corrections for the ground state mass are applied as discussed above. Note that input to the AME from ISOLTRAP are frequency ratios; the calculated mass values given in column 2 are given only

for comparison. Column 3 lists values as obtained in the mass adjustment. The percentage quoted in the last column indicates the influence of the Penning trap data on the adjusted mass values, a label “U” marks those measurements that have not been used in the adjustment because of their larger error compared to the literature values. All data for the nuclides $^{182-185,187-190,192}\text{Hg}$, $^{196,198}\text{Pb}$ that were estimated from systematic trends in [15] are now replaced by ISOLTRAP values. The nuclides $^{186,191,193-195}\text{Hg}$, ^{197}Bi , ^{197}Po and ^{203}At , for which Ref. [15] lists experimental values, now have significantly reduced errors. The mass values of the isotopes $^{196,197,200}\text{Hg}$ and ^{204}Pb which have not been used in the mass adjustment can be checked against the better known adopted mass values. As can be seen perfect agreement is obtained which confirms once more the reliability of the ISOLTRAP measurements.

5 Discussion of results

By integrating the measured frequency ratios into the network of mass relations, ISOLTRAP data allow one to determine the mass of other nuclides or improve their accuracy. This influence is illustrated in Fig. 2 which depicts experimental two-neutron separation energies S_{2n} for the elements Ho ($Z = 67$) to Ac ($Z = 89$) as a function of neutron number. In addition to the results from the Mass Evaluation S_{2n} -values of $^{180,182}\text{Hg}$ based on the results from run #5 are shown. The full circles mark S_{2n} -values that were either unknown before or have an error that is reduced by at least a factor of two (42 cases).

Besides the discontinuity at neutron number $N = 126$, caused by the neutron shell closure, the new S_{2n} -values exhibit a smooth behaviour along the individual isotopic chains. A nearly linear trend can be seen around $Z \geq 78$. Near $N = 108-110$ a deviation from this linear trend is observed for Hf, Ta and W isotopes, which was already noticed in [20]. An attempt trying to explain this discontinuity with a shape transition as observed for the heavier Au and Pt isotopes [18] cannot be sustained by the smooth behaviour of the S_{2n} -values in the area of Pt and Hg isotopes. To clarify the extent of these discontinuities mass measurements of Ir and Au in this mass region will clearly be helpful.

It is interesting to examine the region around $Z = 80$ more closely since here nuclear structure effects due to the presence of shape coexistence may show up. These effects on binding energies are expected to cause deviations from the general trend of mass values in the order of few tens of keV. Figures 3 and 4 show the two-neutron separation energies of neutron-deficient Hg, Pt and Po isotopes as a function of neutron number with a linear function subtracted. These reduced values will be named S'_{2n} . In order to visualize deviations from the generally linear behaviour of the S_{2n} -values around neutron numbers $100 \leq N \leq 110$ (midshell), where nuclear shape coexistence is known

a nearly linear decrease whereas they increase again by roughly 200 keV as one proceeds towards ^{178}Hg . A similar behaviour is observed in the case of platinum. The main differences between both pictures are the sudden drop of around 150 keV at ^{186}Pt but also the increase at ^{194}Pt .

In Ref. [2] it has been illustrated, how shape coexistence manifests itself in the observed spectra for even- A neutron-deficient Hg and Pt isotopes. Near neutron number $N = 104$ for Hg and Pt, two bands are observed, one known from the heavier and only slightly oblate-deformed nuclei and a second one which is interpreted as a rotational spectrum of a strongly prolate-deformed nucleus. While the states associated with the strongly deformed nuclear shape of Hg isotopes come down only to about 400 keV above the ground state, similar excitations in the platinum isotopes $^{178-186}\text{Pt}$ are lowered so much that the nucleus even in the ground state prefers the strongly deformed shape.

6 Effect of low-lying intruder states on binding energies

Is there a correlation between these systematics and the observed trend in binding energies? In order to study this question theoretical work has started. In an upcoming publication the global variation of S_{2n} as derived from the semi-empirical mass formula (Bethe-Weizsäcker) as well as the variation along specific series of isotopes will be discussed [22]. There it will also be pointed out that when the S_{2n} values are plotted as a function of the number of valence nucleon pairs N_ν (counting from the nearest closed shells), an almost pure linear dependence results.

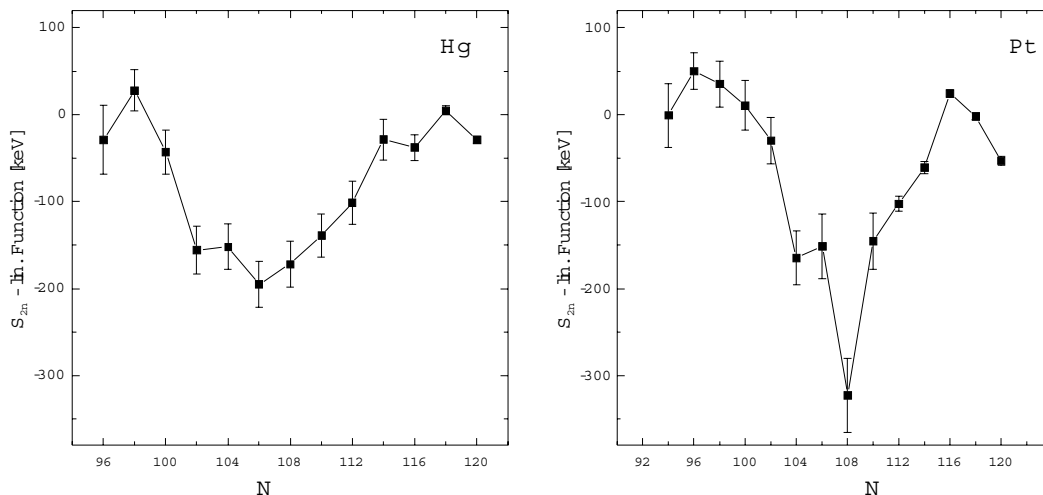


Fig. 3. Reduced S'_{2n} energies for Hg (left) and Pt isotopes (right) as a function of neutron number. The S'_{2n} -values for $^{180,182}\text{Hg}$ include data from the new mass adjustment and from run #5. The data shown for $^{176,178}\text{Pt}$ have been calculated from the mass values of $^{178,180,182}\text{Hg}$ and Q_α -data from [15] (cf. Table 3).

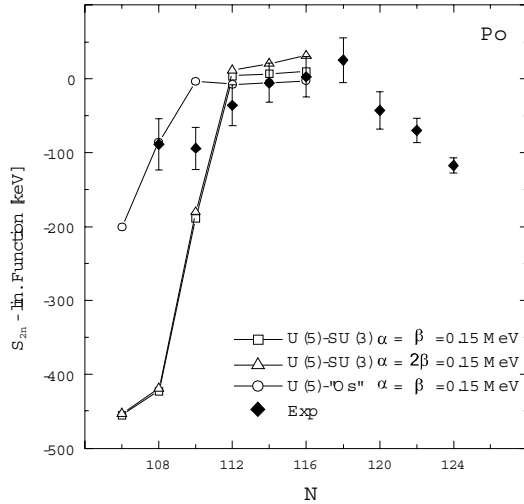


Fig. 4. Reduced S'_{2n} energies for Po isotopes as a function of neutron number. Shown are the experimental values compared with different IBM calculations.

A linear variation of the S_{2n} two-neutron separation energy is obtained in a straightforward way when using a single- j shell and a pure pairing force with strength G . For a degeneracy $\Omega = j + 1/2$, the expression for S_{2n} reads $S_{2n} = G(\Omega - n_\nu + 2)$, with n_ν the number of neutrons filling the j -shell. This seems to be holding to a large extent for the Pb nuclei themselves although one knows that the above approximation cannot hold for a single- j shell with only pairing. The corrections one has to take into account on top of pairing (the major effect though) is the part coming from correlations built into a pure pairing ground state. Taking a proton-neutron quadrupole-quadrupole force as the perturbing force, one can in lowest order evaluate the correction to the pairing binding energy and thus to the S_{2n} two-neutron separation energy [22]. The new expression becomes $S_{2n} = (G + \overline{C})(\Omega - n_\nu + 2) - \overline{C}$. The correction \overline{C} varies between 5 to 20% of the pairing strength G . For a more detailed discussion we refer to [22] where the value of \overline{C} is presented, too.

Very similar linear dependencies are derived starting from an interacting boson model description of the interaction of valence protons and neutrons outside of a closed shell core [21]. Even taking the extra nuclear structure correlations into account that appear in the various dynamical symmetry limits (U(5),SU(3),O(6)), the variation in the two-neutron separation energy S_{2n} remains a linear function of the number of valence nucleon pairs N_ν [23]. Because the parameters appearing in the dynamical symmetry Hamiltonian essentially express the quadrupole strength κ , which itself has some smooth dependence on the number of neutrons, a slight variation in the slope could show up but the dominant part will come from the bulk properties of the interacting valence nucleons.

Any specific local variation in S_{2n} two-neutron separation energies therefore will signal the presence of extra correlation energy in the ground state. The

three possibilities that might be responsible are (i) the presence of a dominant shell closure, (ii) the onset of a hitherto unknown region of deformation and (iii) specific interactions between low-lying intruder states and the ground state that cause a local increase in ground state binding energy.

The data in the Pb region (Pb, Po,... Hg, Pt) are situated below the $N = 126$ shell closure so the only two remaining effects should be studied in more detail. Calculations studying the potential energy landscape (spherical, oblate and prolate deformed configurations) have been carried out recently by R. Wyss et al. [22,24] using a deformed Woods-Saxon potential and by T. Werner et al. [25] using a deformed Hartree-Fock approach.

We carried out studies within the interacting boson model approach in which low-lying intruder configurations are allowed to mix with the regular ground state configuration. Calculations were performed for the Po nuclei with the aim of understanding the rapid lowering of an excited 0^+ state and the band on top of that [26,27]. Using a U(5)-SU(3) dynamical symmetry coupling (ds) and also a more general IBM-1 Hamiltonian for the intruder excitations (g), we studied the influence of mixing on the ground state binding energy and thus on the S_{2n} values. As can be seen from Fig. 4, the overall trend is rather well reproduced and in the lightest Po nucleus where data are obtained, albeit with a large error bar, a local drop of about 400 to 150 keV results, depending on how states are mixing (for more details see [22,27]).

In the Pb nuclei, no specific structure effects show up outside of a linear variation in S_{2n} , up to about mid-shell ($N = 104$). This is consistent with the excitation energy of the lowest 0^+ intruder state not dropping below 0.5 MeV. The measured very slow E0 decay rates in the Pb nuclei [28] are consistent with no or very weak mixing into the ground state and thus no local binding energy increase. Calculations in the Pt nuclei [29] and IBM mixing calculations in the Po nuclei [26,27] may well account for the observed data in the region where the two different families of states come close and interact with mixing matrix elements for the 0^+ states varying between 50 and 200 keV [26]. There appears a problem still when passing the mid-shell (at $N = 104$) to treat excited-state energies and binding energies consistently (related to counting valence nucleons as hole pairs between $N = 126$ and $N = 104$ and as particle pairs, once beyond $N = 104$, counting from $N = 82$). Work on this point is in progress [30].

Independent studies that have attempted to extract the mixing matrix element between the ground state and intruder band members all come close to this value of 50-200 keV as mixing matrix element giving a consistent explanation. More details will be discussed elsewhere [22,23,30].

Even though, at present, it is not possible to derive very precisely every sin-

gle detail of the local S_{2n} -variations, all studies and the various results on ground-to-intruder band state mixing, point towards the interpretation that it is a localized interaction between the ground state and the specific low-lying intruder 0^+ states that is at the origin of the observed effects. Moreover, there is a clear correlation between the energy where the ground state and intruder states have closest approach and the maximal deviation in S_{2n} from a linear variation.

Acknowledgements

This work was supported by the European Commission within the EURO-TRAPS network under contract number ERBFMRXCT97-0144, within the RTD project EXOTRAPS under contract number ERBFMG CET980099 and by NSERC of Canada. We thank R. Wyss for communicating TPE calculations of absolute binding energies prior to publication. Four of the authors (C.D.C, K.H., R.F., J.-E.G.-R.) are most grateful to P. VanIsacker and A. Oros for many discussions on this point. They thank the FWO for financial support and NATO for the research grant CRG96-0981.

References

- [1] K. Heyde et al., Phys. Rep. 102 (1983) 291.
- [2] J. L. Wood et al., Phys. Rep. 215 (1992) 101.
- [3] J. Bonn et al., Phys. Lett. B 38 (1972) 308.
- [4] T. Kühn et al., Phys. Rev. Lett. 39 (1977) 180.
- [5] S. Frauendorf and V. V. Pashkevich, Phys. Lett. B 55 (1975) 365.
- [6] D. Kolb and C. Y. Wong, Nucl. Phys. A 245 (1975) 205.
- [7] M. P. Bradley et al., Phys. Rev. Lett. 83 (1999) 4510.
- [8] G. Bollen et al., Nucl. Instr. and Meth. A 368 (1996) 675.
- [9] H. Raimbault-Hartmann et al., Nucl. Instr. and Meth. B 126 (1997) 378.
- [10] F. Herfurth et al., submitted to Nucl. Instr. and Meth. (2000), preprint CERN-EP/2000-062.
- [11] T. Radon et al., Nucl. Phys. A 677 (2000) 75.
- [12] M. König et al., Int. J. Mass Spectr. Ion. Proc. 142 (1995) 95.

- [13] G. Audi, O. Bersillon, J. Blachot and A. H. Wapstra, Nucl. Phys. A 624 (1997) 1.
- [14] G. Bollen et al., Phys. Rev. C 46, (1992) R2140.
- [15] G. Audi and A. H. Wapstra, Nucl. Phys. A 595 (1995) 409.
- [16] C. Bourgeois et al., Nucl. Phys. A 386 (1982) 308.
- [17] P. Kilcher et al., AIP Conference Proceedings 164 (1987) 517.
- [18] G. Audi and A. H. Wapstra, Nucl. Phys. A 565 (1993) 193.
- [19] G. Audi et al., Nucl. Phys. A 378 (1982) 443.
- [20] R. C. Barber et al., Phys. Rev. Lett. 31 (1973) 728 .
- [21] F. Iachello and A. Arima, The Interacting Boson Model (Cambridge University Press, Cambridge, 1987).
- [22] C. DeCoster et al., to be published.
- [23] J.-E. Garcia-Ramos, C. D. Coster, R. Fossion and K. Heyde, to be published.
- [24] R. Wyss, private communication.
- [25] T. Werner et al., to be published.
- [26] A. Oros et al., Nucl. Phys. A 645 (1999) 107.
- [27] C. DeCoster et al., Nucl. Phys. A 651 (1999) 31.
- [28] P. van Duppen et al., Phys. Rev. Lett. 52 (1984) 1974.
- [29] M. K. Harder, K. T. Tang and P. van Isacker, Phys. Lett. B 405 (1997) 25.
- [30] J.-E. Garcia-Ramos, private communication and to be published.